Video Article

Fabrication of Nano-engineered Transparent Conducting Oxides by Pulsed Laser Deposition

Paolo Gondoni[1], Matteo Ghidelli[1], Fabio Di Fonzo[1,2], Andrea Li Bassi[1,2], Carlo S. Casari[1]

[1]Department of Energy and NEMAS - Center for NanoEngineered Materials and Surfaces, Politecnico di Milano

[2]Center for Nano Science and Technology, Instituto Italiano di Tecnologia

Correspondence to: Carlo S. Casari at carlo.casari@polimi.it

URL: https://www.jove.com/video/50297
DOI: doi:10.3791/50297

Keywords: Materials Science, Issue 72, Physics, Nanotechnology, Nanoengineering, Oxides, thin films, thin film theory, deposition and growth, Pulsed laser Deposition (PLD), Transparent conducting oxides (TCO), Hierarchically organized Nanostructured oxides, Al doped ZnO (AZO) films, enhanced light scattering capability, gases, deposition, nanoporus, nanoparticles, Van der Pauw, scanning electron microscopy, SEM

Date Published: 2/27/2013

Citation: Gondoni, P., Ghidelli, M., Di Fonzo, F., Li Bassi, A., Casari, C.S. Fabrication of Nano-engineered Transparent Conducting Oxides by Pulsed Laser Deposition. *J. Vis. Exp.* (72), e50297, doi:10.3791/50297 (2013).

Abstract

Nanosecond Pulsed Laser Deposition (PLD) in the presence of a background gas allows the deposition of metal oxides with tunable morphology, structure, density and stoichiometry by a proper control of the plasma plume expansion dynamics. Such versatility can be exploited to produce nanostructured films from compact and dense to nanoporous characterized by a hierarchical assembly of nano-sized clusters. In particular we describe the detailed methodology to fabricate two types of Al-doped ZnO (AZO) films as transparent electrodes in photovoltaic devices: 1) at low O_2 pressure, compact films with electrical conductivity and optical transparency close to the state of the art transparent conducting oxides (TCO) can be deposited at room temperature, to be compatible with thermally sensitive materials such as polymers used in organic photovoltaics (OPVs); 2) highly light scattering hierarchical structures resembling a forest of nano-trees are produced at higher pressures. Such structures show high Haze factor (>80%) and may be exploited to enhance the light trapping capability. The method here described for AZO films can be applied to other metal oxides relevant for technological applications such as TiO_2, Al_2O_3, WO_3 and Ag_4O_4.

Video Link

The video component of this article can be found at https://www.jove.com/video/50297/

Introduction

Pulsed Laser Deposition (PLD) employs laser ablation of a solid target which results in the formation of a plasma of ablated species which can be deposited on a substrate to grow a film (see **Figure 1**) [1]. Interaction with a background atmosphere (inert or reactive) can be used to induce homogeneous cluster nucleation in the gas phase (see **Figure 2**) [2,3]. Our strategy for material synthesis by PLD is based on the tuning of material properties in a bottom-up approach by carefully controlling the plasma dynamics generated in the PLD process. Cluster size, kinetic energy and composition can be varied by a proper setting of deposition parameters which affect film growth and result in morphological and structural changes [4,5]. By exploiting the method described here we demonstrated, for a number of oxides (*e.g.* WO_3, Ag_4O_4, Al_2O_3 and TiO_2), the capability to tune morphology, density, porosity, degree of structural order, stoichiometry and phase by modifying the material structure at the nanoscale [6-11]. This allows the design of materials for specific applications [12-16]. With reference to photovoltaic applications, we synthesized nanostructured TiO_2 hierarchically organized by assembling nanoparticles (<10 nm) in a nano- and mesostructure that resembles a 'forest of trees' [13] showing interesting results when employed as photoanodes in dye sensitized solar cells (DSSC) [17]. Based on these previous results we describe the protocol for the deposition of Al-doped ZnO (AZO) films as a transparent conducting oxide.

Transparent conducting oxides (TCOs) are high bandgap (>3 eV) materials converted into conductors by heavy doping, displaying resistivity $<10^{-3}$ ohm-cm and more than 80% optical transmittance in the visible range. They are a key element for many applications such as touch screens and solar cells [18-21] and they are typically grown by different techniques such as sputtering, pulsed laser deposition, chemical vapour deposition, spray pyrolysis and with solution-based chemical methods. Among TCOs, indium-tin-oxide (ITO) has been widely studied for its low resistivity but suffers from the drawback of the high cost and low availability of indium. Research is now moving towards indium-free systems such as F-doped SnO_2 (FTO), Al-doped ZnO (AZO) and F-doped ZnO (FZO).

Electrodes capable of providing an intelligent management of the incident light (light trapping) are particularly interesting for photovoltaic applications. To exploit the possibility to scatter visible light via structures and morphologies modulated at a scale comparable to the wavelength of light (*e.g.* 300-1,000 nm), a good control on the film morphology and on cluster assembly architectures is needed.

In particular we describe how to tune morphology and structure of AZO films. Compact AZO deposited at low pressure (2 Pa oxygen) and at room temperature is characterized by low resistivity (4.5×10^{-4} ohm cm) and visible light transparency (> 90%) which is competitive with AZO

deposited at high temperatures, while AZO hierarchical structures are obtained by ablating at O_2 pressures above 100 Pa. These structures display a strong light scattering capability with haze factor up to 80% and more [22,23].

Protocol

1. Substrate Preparation

1. Cut 1 cm x 1 cm silicon substrates from a Si wafer, Silicon is good for SEM characterization (plane view and cross section).
2. Cut 1 cm x 1 cm glass (soda-lime, 1 mm thick), glass is optimal for optical and electrical characterization.
3. If contacts are needed on glass substrates, Au contacts can be evaporated in vacuum by using a mask. Deposit 10 nm of Cr as an interlayer to improve adhesion of Au, deposit 50 nm of Au.
4. Cut 1 cm x 1 cm polymer sample (*e.g.* Ethylene Tetrafluoroethylene, ETFE).
5. Clean the substrates by sonicating in isopropanol for 5-10 min and rinse in isopropanol, dry using a N_2 flow.

2. Laser Alignment and Selection of Laser Parameters

1. Warm-up the Nd:YAG laser and select IV harmonic emission (266 nm wavelength) by using a fourth harmonic generator (FHG) constituted by two second harmonic generators (SHG) in cascade.
2. Mount a 2%wt. Al_2O_3:ZnO circular target (2" diameter) on the target manipulator. Align the laser spot at the center of the target, start target rotation and translation and set the maximum vertical range. Check that the laser spot never touches the external steel ring used to fix the target. The target is moved with a roto-translational motion to have uniform ablation of the whole target surface.
3. Select repetition rate (*e.g.* 10 Hz) and pulse energy (*e.g.* 75 mJ). Adjust pulse energy and monitor laser stability by a power meter.
4. Move the focusing lens to a selected position and use a piece of sensitive paper attached to the target to measure the spot size. For any position of the focusing lens fire 1-5 laser shots on the paper. Select a lens position to have a laser fluence of about 1 J/cm^2.

3. Setting up PLD and Selection of Deposition Parameters

1. Alignment of substrate position
    1. Mount a circular paper sheet about 2" diameter as a substrate for alignment tests.
    2. Move the substrate holder to a target-to-substrate distance d_{TS} = 50 mm.
    3. Start pumping down the chamber with primary and turbomolecular pumps until the vacuum level reaches 10^{-2} Pa.
    4. Select a gas type (*i.e.* oxygen) and adjust pumping speed and gas flow to have the proper gas pressure (see sections 4 and 5). Adjust x-y position of the substrate manipulator off-axis with respect to the plume center to obtain uniform film thickness over a circular corona.
    5. Start ablation by removing the beam stopper/power meter. If the target is new or if it was not used for long time, this pre-ablation is necessary to clean the target.
    6. Stop ablation when a deposit can be seen on the paper looking from a viewport.

2. Determination of plasma plume length
    1. Follow steps 3.1.1. to 3.1.5, during ablation take pictures with a digital camera with 0.5 - 1 sec accumulation time to average over different plasma plumes.
    2. Measure the visible plasma plume length from the pictures taking d_{TS} as a reference (see **Figure 3**).

3. Calibration of the film thickness
    1. Move the substrate far from the target (*i.e.* 100 mm and more) and move the Quartz Micro-Balance (QCM) at a distance equal to d_{TS} from the target.
    2. Deposit 1000 laser shots (*i.e.* 1' 40") and measure the deposited mass value, then move the QCM away.
    3. Mount a Si substrate as in 1.1.
    4. Deposit a test sample (*e.g.* 18,000 laser shots, *i.e.* 30') and use cross sectional SEM images to calibrate the deposition rate (nm/pulse).

4. Deposition of Nanoengineered AZO Films

1. Mount the substrates prepared as in section 1 on the sample holder manipulator by using adhesive tape.
2. Follow steps 3.1.2 - 3.1.3.
3. Start substrate rotation.
4. Deposition of compact AZO films
    1. Switch on the ion gun and set ion energy at 100 eV, RF power at 75-100 W and Ar gas flux at 20 sccm (the pressure is in the 10^{-2} Pa range). Clean substrates with Ar^+ ion gun for 5-10 min. After the cleaning treatment close gas inlet and pump down the chamber to remove Argon.
    2. Insert oxygen gas and adjust pumping speed and gas flux to have 2 Pa oxygen.
    3. start ablation and deposit for 18,000 shots (30'). During ablation check that the plume length is the same as determined in step 3.2.
    4. stop ablation, close gas inlet, pump down the chamber.

5. Deposition of hierarchically structured AZO films
    1. Insert oxygen gas and adjust pumping speed and gas flow to have 160 Pa oxygen.

2. start ablation and deposit for 18,000 shots (30'). During ablation check that the plume length is the same as determined in step 3.2.
3. stop ablation, close gas inlet, pump down the chamber.

6. Vent the chamber and remove samples

5. Electrical and Optical Characterization

1. Measure the in-plane transport properties using four-probe techniques (*i.e.* Van der Pauw method). See **Figure 4** for a scheme of the contacts. Typical values of the probe current are in the 1 μA to 10 mA range. The measurements is performed over a sample area reduced to 0.7 cm x 0.7 cm to ensure a better thickness uniformity (about 5%).
2. Measure the optical transmittance of the sample and of the bare substrate. Correct the spectra for the substrate contribution by setting to 1 the intensity at the glass/film interface. For a precise correction procedure make sure that the sample is mounted with the glass substrate facing the incident beam. Determine the visible light transparency by calculating the average transmittance in the 400-700 nm range. Use a 150 mm diameter integrating sphere to measure the scattered fraction of the light, the Haze factor can be calculated by dividing the scattered fraction by the total transmitted light (*i.e.* scattered and forward transmitted), see **Figure 5**.

Representative Results

The deposition of AZO by PLD in oxygen atmosphere produces compact transparent conducting films at low background gas pressure (*i.e.* 2 Pa) and mesoporous forest-like structures constituted by hierarchically assembled clusters at high pressures (*i.e.* 160 Pa). The material is constituted by nanocrystalline domains whose size is maximum (30 nm) at 2 Pa [22].

Due to collisions between the ablated species and the background gas, the shape and length of the plasma plume varies significantly with the oxygen pressure in the chamber. (See scheme in **Figure 2** and photographs in **Figure 3**). As a consequence of these phenomena, two deposition regimes can be identified: at low pressures (<10 Pa) film growth takes place in an atom-by-atom, high deposition kinetic energy fashion, resulting in compact films with a columnar structure orthogonal to the substrate surface (**Figure 6**). At high pressures (>10 Pa), nanosized clusters nucleate in the gas phase and impinge on the substrate with lower kinetic energy due to collisions within the plume: the clusters build up porous hierarchical structures resembling a nano-forest (**Figure 6**).

Performing the deposition in oxygen also allows control of stoichiometry in the film: at low deposition pressures a significant amount of oxygen vacancies provides the material with conduction electrons. At an optimal deposition pressure of 2 Pa, where carrier mobility is highest, electrical resistivity is about 5 x 10^{-4} Ω cm. Such material is competitive for application as compact TCO, due to its high visible transparency (85%, average value in the range 400-700 nm), in spite of room temperature deposition (see **Figure 7**).

At high pressures, local stoichiometry order is achieved and the material is characterized by a small concentration of defects, which improves visible transparency (>90%). Furthermore, the mesoscale porosity of samples grown at high pressure maximizes light scattering in the wavelength range of interest (300-1,000 nm) resulting in a haze factor (scattered-to-transmitted photon ratio) over 85% in the range 400-700 nm (**Figure 7**). The electrical properties are strongly related to deposition parameters (*i.e.* oxygen pressure). Moving from compact to nanoporous films, an increase in resistivity is observed, mainly due to the lower degree of film connectivity. As a result, porous films grown at oxygen pressure higher than 100 Pa show low conductivity (resistivity is of the order of 10^6 Ω cm) and thus need further optimization. To improve the conductivity a possible strategy is represented by growing the films in mixed gas atmospheres (Ar:O_2) to obtain an independent control of morphology and stoichiometry. Using a total pressure of 100 Pa (Ar partial pressure of 98 Pa and O_2 partial pressure of 2 Pa) allows to obtain film resistivities of the order of 100 Ω cm.

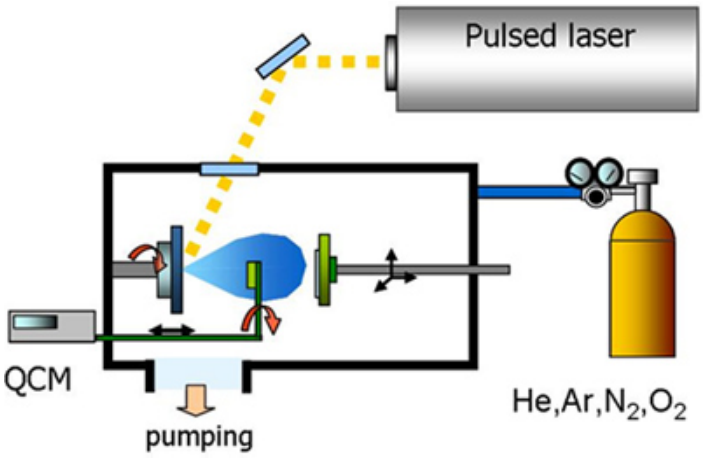

Figure 1. Scheme of the pulsed laser deposition apparatus.

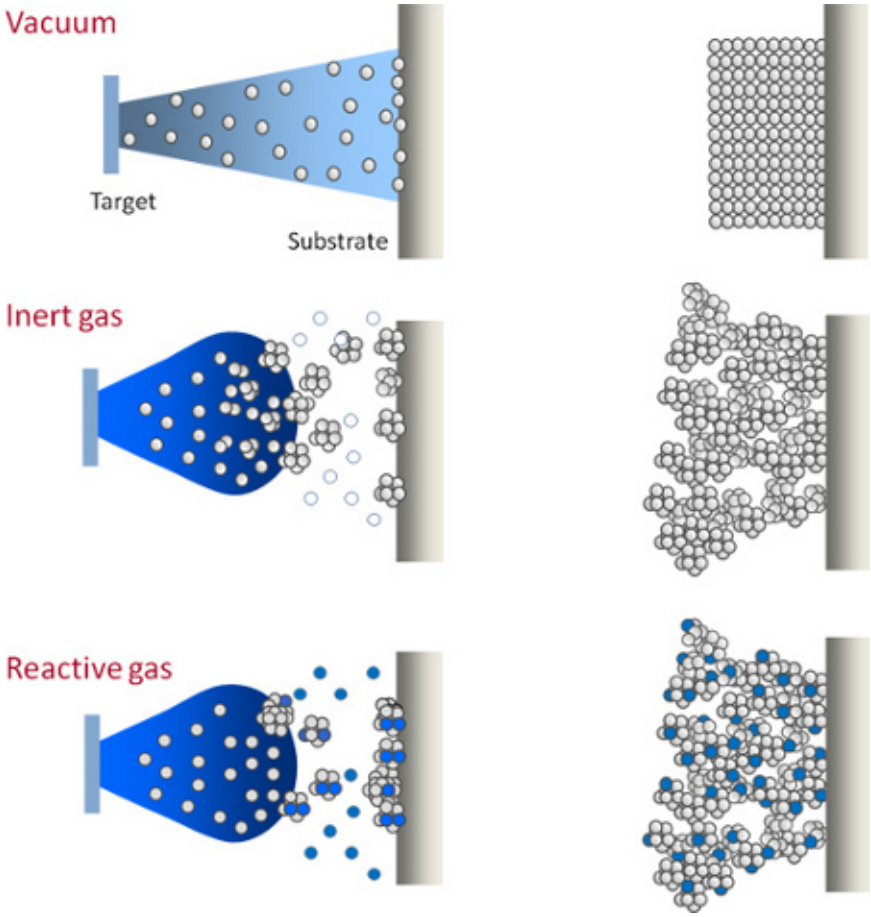

Figure 2. Pictorial view of the deposition process in vacuum and in the presence of inert and reactive gases.

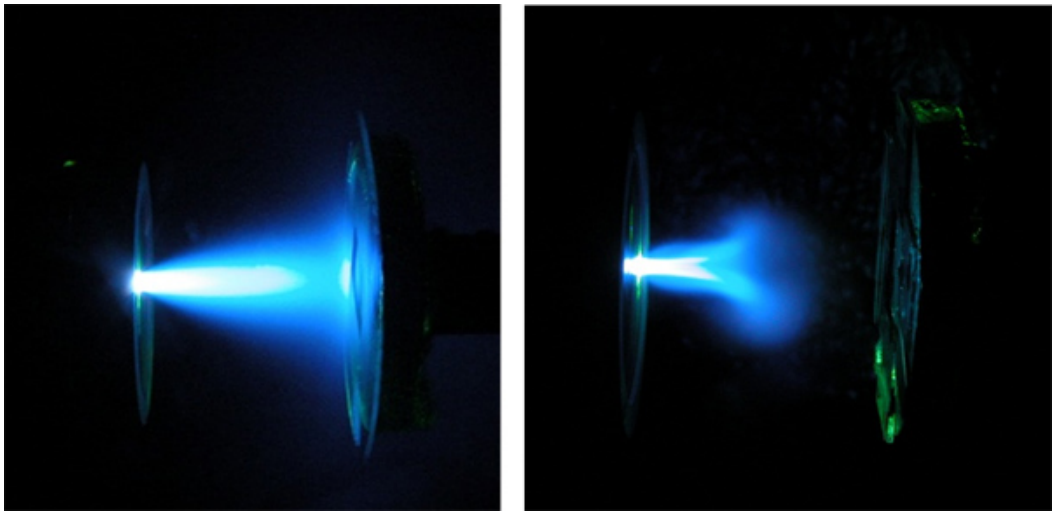

Figure 3. Pictures of the plasma plume at 2 Pa oxygen (left) and at 160 Pa oxygen (right). The target to substrate distance is 50 mm.

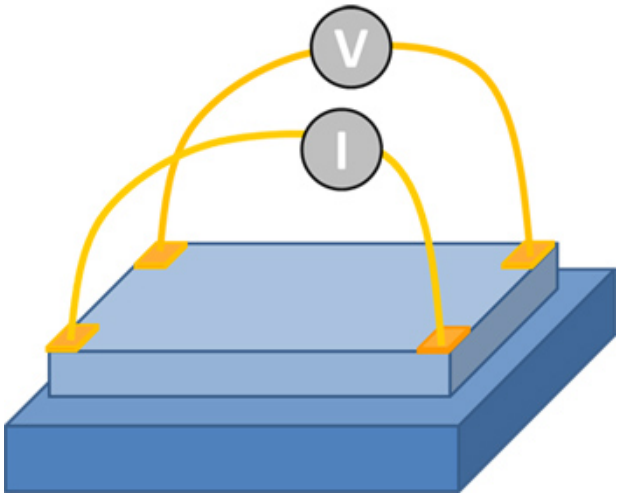

Figure 4. Scheme of the contacts for four point probe electrical measurements (Van der Pauw).

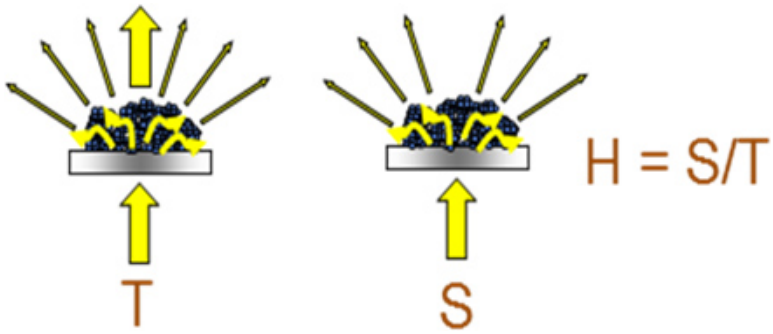

Figure 5. Schematic representation of the measurement of the Haze factor (H); T is the total transmitted light (forward and scattered transmitted light) and S is the scattered component.

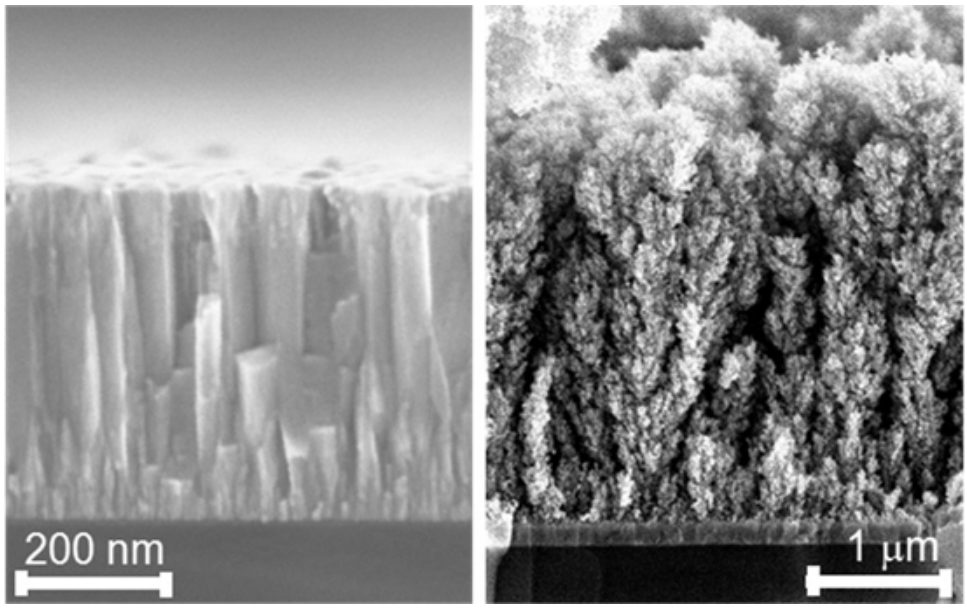

Figure 6. Cross sectional SEM pictures of AZO films deposited at 2 Pa oxygen (left) and 160 Pa oxygen (right) for 30 min.

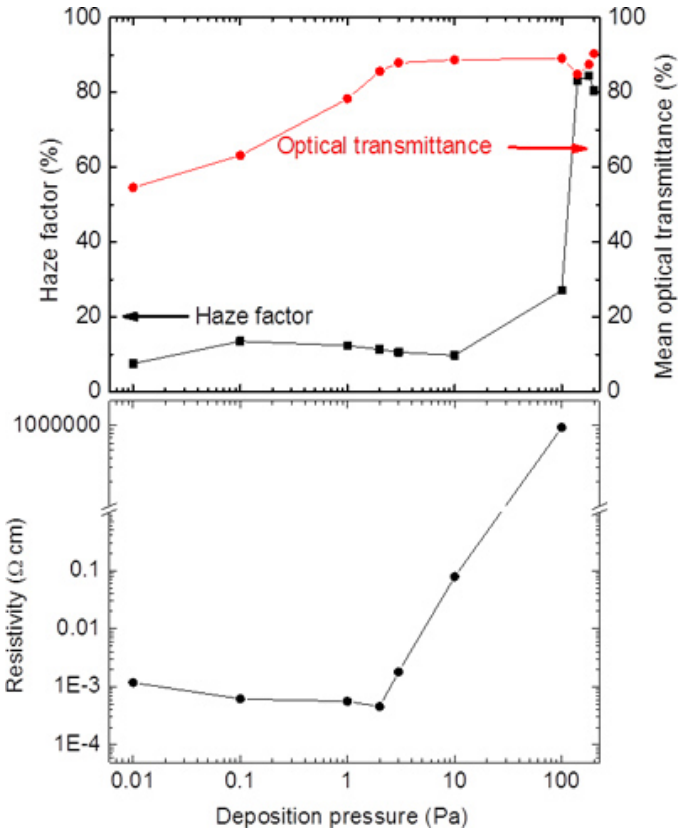

Figure 7. Optical transmittance (average value in the 400 nm - 700 nm range) and Haze factor (top) and electrical resistivity (bottom) as a function of oxygen background pressure.

Discussion

The plasma plume shape is closely related to the ablation process, especially in the presence of a gas; monitoring the plasma plume by visual inspection is important to control the deposition. When depositing a metal oxide by ablating an oxide target, oxygen is needed to support oxygen losses during the ablation process. At lower oxygen background gas pressure, the deposited material may have oxygen vacancies. This effect is reduced by increasing the gas pressure. To separate stoichiometry from morphology gas mixtures (*i.e.* Ar:O_2 or He:O_2) can be used: inert gas to tune morphology, reactive gas to tune composition and stoichiometry. PLD in vacuum or at low background gas pressure (typically less than a few Pa) usually leads to high kinetic energy deposition of the ablated species (*i.e.* up to hundreds of eV/atom). This may result in the accumulation of internal stress which can eventually lead to film delamination. In the case of AZO we found that the substrate bombardment with Ar ions (step 4.4.1) prior to deposition is fundamental to avoid such problems. On the contrary, delamination is not an issue for nanoporous films due to the lower energy deposition regimes occurring at higher background gas pressures and the corresponding growth of an open porous film structure.

The methodology proposed here can be used for other metals and metal oxides [24]. One of the most critical parameters, when ablating in the presence of a background gas, is the relative position of the substrate with respect to the visible plasma plume length. The visible plume length, as it can be measured from digital pictures, corresponds to the maximum distance reached by the shock front during plasma expansion [25]. Conditions for the formation of a shock front depend on the ablated material, laser fluence and gas type and pressure. The typical plume shape with a well defined edge, as shown for instance in **Figure 3** (right), is an example of shock front formation. More compact morphologies can be obtained by selecting a substrate-to-target distance shorter than the plume length, while more open and porous films are obtained with a substrate-to-target distance longer than the plume length [6].

Possible limitations are related to the maximum sample area. Without substrate motion the typical sample area is up to 2 cm x 2 cm. By a proper off-axis rotation of the substrate holder, sample areas up to 4 cm x 4 cm or 3 cm x 3 cm with a good uniformity (thickness variation within 10%) can be produced [26]. A similar uniformity was obtained on AZO films (*i.e.* 10% for 1cmx1cm). The deposition rate is strongly dependent on the deposition parameters, in the present case the growth rate of AZO with a rotating substrate holder was about 14 nm/min for compact films and 50 nm/min for porous ones. Such values are related to a laser repetition rate of 10 Hz and can be increased by one order of magnitude with a 100 Hz repetition rate. The deposition is performed at room temperature and we do not observe any substrate heating. Thanks to this a wide range of substrates can be used, and in addition to silicon and glass we successfully deposited AZO on plastic (*i.e.* Ethylene tetrafluoroethylene, ETFE) [27]. Another potential criticality is related to the mechanical stability of the nanoporous structures. As-deposited samples should be managed with care taking into account that the mechanical stability decreases with increasing the background gas pressure used during the PLD process. In the case of AZO, the low stability of porous films made a proper contact with the electrical probes extremely difficult. Generally, mechanical stability can be improved by thermal annealing treatments at 400-500 °C in air or in inert gases without substantially modify the overall morphology, as shown for both for AZO and TiO_2 [7,23].

In conclusion our method allows to deposit both compact and nanoporous AZO films with a fine control of the structural and morphological properties. Compact films show competitive functional properties in terms of transparency to the visible light and electrical conductivity. Nanoporous films consisting in hierarchically organized structures from the nano- to the micro-scale, resembling a forest of trees, assure very efficient scattering capability of the incident light (high haze factor) thus opening the possibility to develop electrodes with light trapping functionality. The proposed methodology is not only related to the deposition of AZO but can be also applied to other metals and oxides. The properties of compact and porous films can be combined by growing multilayered or graded films, in order to obtain a multiply functionalized material.

Disclosures

No conflicts of interest declared.

References

1. Chrisey, D.B., Hubler, G.K., eds., Pulsed Laser Deposition of Thin Films, John Wiley & Sons, New York, (1994).
2. Lowndes, D.H., Geohegan, D.B., Puretzky, A.A., Norton, D.P., & Rouleau, C.M. Synthesis of novel thin-film materials by pulsed laser deposition. *Science.* **273**, 898 (1996).
3. Di Fonzo, F., Bailini, A., Russo, V., Baserga, A., Cattaneo, D., Beghi, M.G., Ossi, P.M., Casari, C.S., Li Bassi, A., & Bottani, C.E. Synthesis and characterization of nanostructured tungsten and tungsten oxide films. *Catalysis Today.* **116**, 69-73 (2006).
4. Casari, C.S., Foglio, S., Passoni, M., Siviero, F., Bottani, C.E., & Li Bassi, A. Energetic regimes and growth mechanisms of pulsed laser deposited Pd clusters on Au(111) investigated by *in situ* Scanning Tunneling Microscopy. *Physical Review B.* **84**, 155441 (2011).
5. Cattaneo, D., Foglio S., Casari, C.S., Li Bassi, A., Passoni, M., & Bottani, C.E. Different W cluster deposition regimes in pulsed laser ablation observed by *in situ* Scanning Tunneling Microscopy. *Surface Science.* **601**, 1892-1897 (2007).
6. Bailini, A., Di Fonzo, F., Fusi, M., Casari, C.S., Li Bassi, A., Russo, V., Baserga, A., & Bottani, C.E. Pulsed laser deposition of tungsten and tungsten oxide thin films with tailored structure at the nano- and mesoscale. *Applied Surface Science.* **253**, 8130-8135 (2007).
7. Fusi, M., Russo, V., Casari, C.S., Li Bassi, A., & Bottani, C.E. Titanium oxide nanostructured films by reactive pulsed laser deposition. *Applied Surface Science.* **255** (10), 5334-5337 (2009).
8. Dellasega, D., Facibeni, A., Di Fonzo, F., Russo, V., Conti, C., Ducati, C., Casari, C.S., Li Bassi, A., & Bottani, C.E. Nanostructured High Valence Silver Oxide Produced by Pulsed laser Deposition. *Applied Surface Science.* **255** (10), 5248-5251 (2009).
9. Di Fonzo, F., Tonini, D., Li Bassi, A., Casari, C.S., Beghi, M.G., Bottani, C.E., Gastaldi, D., Vena, P., & Contro, R. Growth regimes in pulsed laser deposition of alumina films. *Applied Physics A.* **93** 765-769 (2008).
10. Bailini, A., Donati, F., Zamboni, M., Russo, V., Passoni, M., Casari, C.S., Li Bassi, A., & Bottani, C.E. Pulsed Laser Deposition of Bi2Te3 Thermoelectric Films. *Applied Surface Science.* **254**, 1249-1254 (2007).
11. Baserga, A., Russo, V., Di Fonzo, F., Bailini A., Cattaneo, D., Casari, C.S., Li Bassi, A., & Bottani, C.E. Nanostructured Tungsten Oxide With Controlled Properties: Synthesis And Raman Characterization. *Thin Solid Films.* **515**, 6465-6469 (2007).
12. Dellasega, D., Facibeni, A., Di Fonzo, F., Bogana, M., Polissi, A., Conti, C., Ducati, C., Casari, C.S., Li Bassi, A., & Bottani, C.E. Nanostructured Ag_4O_4 films with enhanced antibacterial activity. *Nanotechnology.* **19**, 475602 (2008).
13. Di Fonzo, F., Casari, C.S., Russo, V., Brunella, M.F., Li Bassi, A., & Bottani, C.E. Hierarchically organized nanostructured TiO_2 for photocatalysis applications. *Nanotechnology.* **20**, 015604 (2009).
14. Torta, F., Fusi, M., Casari, C.S., Bottani, C.E., & Bachi, A. Titanium Dioxide Coated MALDI plate for on target Analysis of Phosphopeptides. *Journal of Proteome Research.* **8**, 1932-1942 (2009).
15. Ponzoni, A., Russo, V., Bailini, A., Casari, C.S., Ferroni, M., Li Bassi, A., Migliori, A., Morandi, V., Ortolani, L., Sberveglieri, G., & Bottani, C.E. Structural And Gas-Sensing Characterization Of Tungsten Oxide Nanorods And Nanoparticles. *Sensors & Actuators: B. Chemical B.* **153**, 340-346 (2011).
16. Li Bassi, A., Bailini, A., Donati, F., Russo, V., Passoni, M., Mantegazza, A., Casari, C.S., & Bottani, C.E. Thermoelectric properties of Bi-Te Films with controlled structure and morphology. *Journal of Applied Physics.* **105**, 124307 (2009).
17. Sauvage, F., Di Fonzo, F., Li Bassi, A., Casari, C.S., Russo, V., Divitini, G., Ducati, C., Bottani, C.E., Comte, P., & Graetzel, M. Bio-inspired hierarchical TiO2 photo-anode for dye-sensitized solar cells. *Nano Letters.* **10**, 2562-2567 (2010).
18. Grankvist, C.G. Transparent conductors as solar energy materials: A panoramic review. *Solar Energy Materials & Solar Cells.* **91**, 1529 (2007).
19. Minami, T. Transparent conducting oxide semiconductors for transparent electrodes. *Semicond. Sci. Technol.* **20**, S35 (2005).
20. Fortunato E., *et al.* Transparent Conducting Oxides for Photovoltaics. *MRS Bulletin.* **32**, 242 (2007).
21. Exarhos, G.J., *et al.* Discovery-based design of transparent conducting oxide films. *Thin Solid Films.* **515**, 7025 (2007).
22. Gondoni, P., Ghidelli, M., Di Fonzo, F., Russo, V., Bruno, P., Mart-Rujas, J., Bottani, C.E., Li Bassi, A., & Casari, C.S. Structural and functional properties of Al:ZnO thin films grown by Pulsed Laser Deposition at room temperature. *Thin Solid Films.* **520**, 4707-4711 (2012).
23. Gondoni, P., Ghidelli, M., Di Fonzo, F., Carminati, M., Russo, V., Li Bassi, A., & Casari, C.S. Structure-dependent optical and electrical transport properties of nanostructured Al-doped ZnO. *Nanotechnology.* **23**, 365706 (2012).
24. Casari, C.S. & Li Bassi, A. In: *Pulsed Laser Deposition of Nanostructured Oxides: from Clusters to Functional Films.* Advances in Laser and Optics Research, Arkin, W.T., ed., Nova Science Publishers Inc., **7**, 65-100 (2012).
25. Amoruso, S., Sambri, A., Vitiello, M., & Wang, X. Plume expansion dynamics during laser ablation of manganates in oxygen atmosphere. *Applied Surface Science.* **252**, 4712-4716 (2006).
26. Uccello, A., Dellasega, D., Perissinotto, S., Lecis, N., & Passoni, M. Nanostructured Rhodium Films for Advanced Mirrors Produced by Pulsed Laser Deposition. *Journal of Nuclear Materials.*, Accepted, doi:10.1016/j.jnucmat.2012.08.046 (2013).
27. Gondoni, P., Ghidelli, M., Di Fonzo, F., Russo, V., Bruno, P., Martí-Rujas, J., Bottani, C.E., Li Bassi, A., & Casari, C.S. Highly Performing Al:ZnO Thin Films grown by Pulsed Laser Deposition at Room Temperature. *Nanoscience and Nanotechnology Letters.*, Accepted, (2013).

